HHS Public Access

Author manuscript

Gene Ther. Author manuscript; available in PMC 2012 December 26.

Published in final edited form as:

Gene Ther. 2011 November ; 18(11): 1043–1051. doi:10.1038/gt.2011.47.

Investigation of the peak action wavelength of light-activated gene transduction (LAGT)

Max Myakishev-Rempel[1,2,4], **Jerry Kuper**[1,2], **Benjamin Mintz**[3], **Sara Hutchinson**[3], **Jay Voris**[2], **Katrina Zavislan**[2], **Sarah Offley**[4], **Frances Barg Nardia**[4], **Zaneb Yaseen**[4], **Tony Yen**[3], **James Zavislan**[2], **Michael D. Maloney**[4], and **Edward M. Schwarz**[1,4,5]

[1]LAGeT LLC, Rochester, NY

[2]Center for Institute Ventures, Institute of Optics, University of Rochester, Rochester, NY

[3]Department of Biomedical Engineering, University of Rochester, Rochester, NY

[4]The Center for Musculoskeletal Research, University of Rochester, Rochester, NY

Abstract

Light-activated gene transduction (LAGT) is an approach to localize gene therapy via preactivation of cells with UV light, which facilitates transduction by recombinant adeno-associated virus vectors. Prior studies demonstrated that UVC induces LAGT secondary to pyrimidine dimer formation, while UVA induces LAGT secondary to reactive oxygen species (ROS) generation. However, the empirical UVB boundary of these UV effects is unknown. Thus, we aimed to define the action spectra for UV-induced LAGT independent of DNA damage, and determine an optimal wavelength to maximize safety and efficacy. Results: UV at 288, 311 and 320nm produced significant dose-dependent LAGT effects, of which the maximum (800-fold) was observed with 4kJ/m^2 at 311nm. Consistent with its robust cytotoxicity, 288nm produced significantly high levels of DNA damage at all doses tested, while 311, 320 and 330nm did not generate pyrimidine dimers and produced low levels of DNA damage detected by comet assay. While 288nm failed to induce ROS, the other wavelengths were effective, with the maximum (10-fold) effect observed with 30 kJ/m^2 at 311nm. An *in vivo* pilot study assessing 311nm-induced LAGT of rabbit articular chondrocytes demonstrated a significant 6.6-fold ($p<0.05$) increase in transduction with insignificant cytotoxicity. Conclusion: 311nm was found to be the optimal wavelength for LAGT based on its superior efficacy at the peak dose, and its broad safety range that is remarkably wider than the other UV wavelengths tested.

[5]To whom correspondence should be addressed: Dr. Edward M. Schwarz, The Center for Musculoskeletal Research, University of Rochester Medical Center, 601 Elmwood Avenue, Box 665, Rochester NY 14642, Phone 585-275-3063, FAX 585-275-1121, Edward_Schwarz@URMC.Rochester.edu.

Conflict of interest

Max Myakishev-Rempel is an employee of LAGeT LLC. Jerry Kuper is a consultant of LAGeT LLC and has equity in the company. Edward Schwarz is President and Founder of LAGeT LLC.

Introduction

One of the promises of gene therapy is local treatment to achieve supra-pharmacological dosing and limit systemic side-effects, which cannot be achieved by traditional small molecule or biologic therapies. While localized gene transfer approaches have been developed via: direct injection of vectors with limited biodistribution, vectors with limited tissue tropism, or tissue specific promoters1–5, currently there is no technology that can site-specifically target gene expression to a limited number of cells within a particular tissue. The development of this technology would greatly facilitate gene therapies for tissue repair and regeneration, which requires a morphogenic gradient to perpetuate unidirectional growth and differentiation, such as that observed in epimorphic regeneration6,7. To the end of site-specific gene therapy, we proposed a light-activated gene transduction (LAGT) approach, which is designed to work with first generation single-stranded recombinant adeno-associated viral vectors (rAAV)4,8. While these vectors have many advantages, including high infection efficiency of multiple non-dividing cell types, rAAV transduction is limited by inefficient second-strand DNA synthesis,8–10 which takes days to weeks to occur in some gene therapies8–13. Based on prior studies that demonstrated that rAAV transduction is enhanced by DNA damaging agents (i.e. short wavelength 254nm UVC) that induce DNA repair enzymes in exposed cells to facilitate second-strand synthesis,9,10,14,15 we demonstrated that the same increased transduction efficiency can be achieved independently of DNA damage via pretreatment with long wavelength UVA (325nm).16 The mechanism responsible for this UV-induced LAGT effect was shown to be the generation of intracellular reactive oxygen species (ROS), which are also known to activate DNA polymerases. While we were unable to detect significant levels of various forms of DNA damage that were directly caused by 325nm UVA exposure, the most common of which is pyrimidine dimer formation, high levels of ROS produced by this treatment are cytotoxic due to membrane lipid-peroxidation. Thus, safe and effective LAGT can be achieved within a window of UV exposures that generates sufficient ROS to activate DNA polymerases, but not above the level that can be resolved by cellular catalases and superoxide dismutase. In the case of articular chondrocytes, this safe and effective exposure window for site-specific LAGT at 325nm UVA is between 600 and 12,000J/m^2 (joule per square meter).16

The feasibility of LAGT for targeted *in vivo* gene therapy is defined by several parameters. The first is the power of the light source (J/m^2/sec), as it is desirable to deliver the effective UV dose in as short a time as possible. Indeed, this drove our initial decision to use 325nm UVA, which can be delivered by a helium-cadmium laser through a collimated fiber-optic cable at a fluence of 330 J/m^2/sec. While proof of principle studies demonstrated that safe and effective LAGT can be achieved with this system,16 several critical questions remain regarding the action spectrum of UV for this approach. Specifically, 1) What is the shortest UV wavelength that does not directly induce DNA damage? 2) What is the longest UV wavelength that mediates the LAGT effect? 3) Which UV wavelength achieves the greatest LAGT effect? And 4) Which UV wavelength has the broadest safety-efficacy window for LAGT? To the end of defining these empirical properties of various UV action spectra, we performed a series of *in vitro* experiments with UVB-UVA wavelengths that spanned from 288nm to 365nm.

Results

Experimental systems

In order to evaluate the empirical properties of a broad range of UV wavelenghts on LAGT efficacy, cytotoxicity, DNA damage and ROS generation, we established three light delivery systems. The first was a xenon short arc light source, fitted with bandpass filters, which were designed to interrogate the UVB to UVA transition. Based on our hypothesis that the optimum wavelength for LAGT would be in the 305–330nm range, we used three different bandpass filters that transmitted bands over this action spectra region with partially overlap in the wings of their bandpass curves. We also used a fourth bandpass filter that transmitted UVB emission at wavelengths below the range of interest. These bandpass filters provided a peak transmission of average 65% at full output power (Table 1), with a full width at measured half maximum bandpass centered at the following wavelengths: 287.7±5.0, 311.4±5.7, 320.5±6.2 and 330.1±4.9nm (Figure 1). Since we had previously determined that longer wavelength UV requires increasingly more energy to mediate LAGT versus short wavelengths,16 and only high power light sources are able to deliver these UV doses to cell cultures in a timely manner, we utilized a frequency shifted Nd:YLF laser and a UV LED light source to evaluate the effects of 349nm and 365nm UVA respectively.

Evaluation of UV wavelengths for their peak LAGT effect

In order to determine the peak LAGT effect of the six UV delivery systems, we determined the transfection efficiency of rAAV-luciferase (Luc) following infection of two different cell lines. The first, C3H10T.5 cells (C3H), is a murine mesenchymal progenitor that is representative of cell lines that are not easily transfected with single-stranded rAAV vectors. The second, 293 cells, were derived from human embryonic kidney, and is representative of cell lines that are highly transfectable by rAAV vectors. Figure 2 illustrates the dose-dependent LAGT effects of the UV systems focused at 288nm, 311nm and 320nm. Note that each of these systems displayed a biphasic response in which a dose-dependent peak increase in transduction was followed by a dramatic loss of LAGT at higher doses, which is consistent with an exposure window that lies between efficacy and cytotoxicity. Among these, both the 311nm and 320nm systems demonstrated remarkable peak LAGT effects that were >750-fold in C3H and >150-fold in 293 cells. Also of note are the low doses that generated these peaks, 13kJ/m^2 and 100kJ/m^2, delivered in 30 and 180 seconds for the 311nm and 320nm systems, respectively. We also performed broad UV dose-response experiments with the 330nm, 349nm and 365nm systems, which failed to demonstrate significant LAGT effects at all fluences tested (Figure 2 and data not shown). While this result was not surprising for the very long wavelength UVA systems, the lack of LAGT effect with the 330nm system demonstrates that the longest wavelength that can be used for this technology is ~325nm, which we previously demonstrated to mediate a modest 8-fold peak LAGT effect.16

Evaluation of UV wavelengths for their cytotoxicity and genotoxicity

In order to assess UV effects on cytotoxicity we performed *in situ* trypan blue staining on C3H and 293 cells exposed to various doses of light delivered by the 288nm, 311nm, 320nm and 330nm systems (Figure 3). All 4 wavelengths induced dose-dependent cell death.

288nm UV was the most cytotoxic, reaching 100% cell death at 9 kJ/m^2 (C3H cell line), while the longer wavelengths were less toxic. Surprisingly, 311nm UV was the least cytotoxic, and only killed less than 13% of the cells at over twice the peak LAGT dose.

Our initial attempts at measuring macromolecular UV-induced DNA damage from double-strand breaks via fragmentation of genomic DNA assessed by gel electrophoresis failed to demonstrate remarkable effects for all wavelengths tested (data not shown). Therefore, we repeated these exposures and assessed UV-induced DNA damage via the single cell gel electrophoresis Comet assay, which is a more sensitive technique that detects both double and single-stranded DNA breaks, the majority of apurinic sites, apyrimidinic sites, as well as alkali-labile DNA adducts such as phosphoglycols and phosphotriesters.17,18 The results from this experiment with 288nm, 311nm, 320nm and 330nm UV are presented in Figure 4. Consistent with the cytotoxicity data, 288nm UV produced the most DNA damage; 320nm UV also produced significant DNA damage in a dose dependent manner in C3H cells, but did not have these significant effects in 293 cells. Remarkably, neither 311nm nor 330nm UV induced significant comet tails in this assay.

As pyrimidine dimmer formation is the most prominent DNA modification induced by UV exposure, we determined the ability of 288nm, 311nm, 320nm and 330nm UV to generate these genetic lesions by ELISA. The results of this experiment demonstrated that only 288nm UV is capable of inducing high levels of pyrimidine dimers (Figure 5). While 64kJ/m^2 of 320nm UV did induce very low levels of pyrimidine dimers, 311nm and 330nm UV were unable to induce levels above that observed in the no-UV treatment controls. Collectively, these results demonstrate that in contrast to high levels of 288nm UV-induced cytotoxicity and DNA damage at the low end of the UVB range, 311nm at the high end of the UVB range has a very favorable safety profile for LAGT.

Evaluation of UV wavelengths for their ability to induce ROS

Since UVA-induced LAGT independent of DNA damage is mediated by the generation of intracellular ROS, we examined the ability of 288nm, 311nm, 320nm and 330nm UV to induce intracellular ROS via detection of fluorescent dichlorofluorescein diacetate (DCFH-DA) by flow cytometry. The results from this experiment demonstrated that only 311nm UV induced intracellular ROS at all doses tested in both cell lines (Figure 6). In contrast, 288nm UV failed to induce ROS levels above background at all doses tested, while 320nm and 330nm only significantly increased ROS levels in 293 cells, but not in C3H cells. Taken together with the results from the LAGT, cytotoxicity and DNA damage data, these results clearly demonstrate that 311nm UV has the greatest safety-efficacy window for site-specific gene therapy.

Effects of UV on light-activated gene transduction in vivo

The safety and efficacy and of LAGT for articular cartilage gene therapy was tested *in vivo* using an established rabbit patellar groove defect model.16,19 To assess UV-induced cell death, the right knees of the rabbits were treated with LAGT using 0, 2, 6 and 18 KJ/m^2 of 313 nm UV light (N=4). The tissues were harvested 48 hours later, and cell death was quantified by counting the number of empty lacunae/total lacunae in Safarin-O/Fast green

(SO/FG)-stained sections. The results demonstrated that there was no significant effect of LAGT treatment on articular chondrocyte cell death (0 KJ/m^2 = 0.06±0.05%; 2 KJ/m^2 = 0.06±0.04%; 6 KJ/m^2 = 0.18±0.08%; and 18 KJ/m^2 = 0.59±0.47%; mean ± SEM; $p>0.05$ vs. 0 KJ/m^2 for all doses).

For the efficacy test, the right knees were treated with or without 6 KJ/m^2 of 313 nm UV light, followed by a direct injection rAAV-GFP (N=4). The tissues were harvested 48 hours later and the transduction efficiency was determined by counting eGFP-positive articular chondrocytes in sections process for immunohistochemistry (Figure 7). The results demonstrated a significant increased transduction in the UV treated knees (UV treated = 54.2±14.3%; no UV = 8.2±3.2%; mean ± SEM; $p<0.05$).

Discussion

Gene therapy to facilitate healing of damaged adult-mammalian tissues that have very limited regenerative potential is significantly limited by our inability to target transgene expression to the edge of the defect, in a timely manner, while limiting transduction of the uninjured-healthy tissue. As an example, we have been working towards a gene therapy for articular and meniscal cartilage defects, which are extremely prevalent (>80% of people >50yrs) due to simple sports related injuries, and are known to be the leading cause of osteoarthritis and the need for joint replacement surgery20,21. Based on the biology of cartilage repair in vertebrae-regenerate species, which is highlighted by precise temporal-spatial gene expression at the edge of the defect immediately following injury to establish a morphogenic gradient and blastema formation22,23, we envisioned a gene therapy performed during standard arthroscopy with potential to achieve this requisite gene expression profile. In this surgery, mechanical debridement is performed to remove the fragmented cartilage and stabilize the margins of the defect. This surgical procedure re-establishes the opportunity to initiate formation of new cartilage via creation of morphogenic gradient of chondrogenic factors (i.e. GDF-5) via site-specific gene therapy. LAGT represents one approach that is compatible with standard arthroscopy, and we have previously demonstrated safe and effective LAGT with 325nm UVA in a rabbit articular cartilage defect model16. However, several significant improvements are needed to maximize the potential of LAGT therapy. These improvements require greater understanding of action spectra at the UVB-UVA boundary, which is the focus of the current study.

Biological pathways related to UV damage have been shown to be wavelength dependent 24. The two basic mechanisms for UV induced cellular DNA damage are direct damage and indirect damage through alternative intracellular photosensitizing molecules. For irradiation close to the UVC range (250nm to 300nm), the dominant form of DNA damage is direct excitation that can be traced through pyrimidine dimerization. With longer wavelengths approaching the UVA range (>300nm), damage tends to occur indirectly through the excitation of intracellular chromophores. These chromophores can either be stimulated to damage DNA directly via generation of singlet oxygen species (type I photoreaction from O_2 radicals), or via superoxide/hydroxyl radical formation through Fenton reaction (type II photoreaction)25. This oxidative DNA damage is primarily repaired through the action of

DNA glycosylases, AP endonucleases, and general nucleotide excision repair mechanisms including methylguanine DNA methyl transferase, MGMT activation26. Interestingly, these ROS including superoxide, singlet oxide, and peroxide radicals have been shown to induce activation of ATM kinase and p53 transcription, which are known to play a major role in DNA repair processes without causing DNA damage directly.27 Thus, UVA-induced type I and type II photoreactions provide therapeutic potential if a significant window between cytotoxicity-genotoxicty and efficacy exists, and efforts to identify the empirical windows for various action spectra at the UVB-UVA boundary are warranted.

Consistent with the known direct DNA damage induced by short wavelength UVB, here we demonstrate that 288nm LAGT and cytotoxicity is directly associated with high levels of pyrimidine dimers without ROS generation. In contrast, 311nm effects are associated with significant ROS levels without pyrimidine dimer formation. Furthermore, 311nm failed to induce macroscopic DNA damage as assessed by a Comet assay, demonstrating that these exposures do not induce type I or type II DNA damage either. Given that the empirical cutoff of UVB-induced LAGT independent of DNA damage must fall within the 288nm and 311nm systems, we interpolated this cutoff to be 299±3nm as follows. First, there is a rapid drop off in DNA absorbance at UV wavelengths focusing at 299nm, leading to the complete absence of DNA absorbance above 302nm.28 Since this rapid drop of DNA absorbance coincides with the 299nm border wavelength between the 288nm irradiation system that produced high DNA damage with low ROS, and the 311nm irradiation system that produced low DNA damage with high ROS, and since the irradiation peaks centered at 288nm and 311nm do not overlap, we conclude that the empirical boundary of the action spectra of DNA damage dependent vs. DNA damage independent LAGT to be at 299±3nm.

A major disappointment with the 325nm HeCd laser system we used previously is its modest LAGT effects (8-fold)16. This prompted us to evaluate shorter UVA wavelengths more closely. Remarkably, both 311nm and 320nm UVA achieved 100-fold greater LAGT effects at their peak fluences. Moreover, the 4-fold increased LAGT effect observed in C3H vs. 293 cells is consistent with a greater net activation of host DNA polymerases in the less transfectable cell line. As this effect would be even greater in nondividing cells, the peak LAGT effect in articular chondrocytes could be several thousand fold, and warrants future investigation.

As with most experimental research, our studies produced several results whose explanation is beyond the scope of our current understanding. Most notably are the sharp loss of the LAGT effect at doses 3-fold and 1.5-fold above the peak for 311nm and 320nm UV respectively. As this was not due to a commensurate increase in cytotoxicity, this biphasic response to short wavelength UVA suggests that there may be negative cellular feedback mechanisms that are triggered prior to cell death. Our other enigmatic observation that begs further investigation is the observation that greater cytotoxicity and DNA damage was observed at 320nm compared to 311nm and 330nm. This suggests that a yet to be identified cellular chromophore with a narrow excitation spectrum between 316nm and 325nm exists.

Collectively, our results clearly indicated that the 311nm UVA system is the most ideal light source for LAGT that we have tested to date, based on its ability to generate high levels of

ROS with minimal DNA damage, and cause more than a 800-fold increase in transgene expression in C3H cells. Moreover, we find this 311nm system to be a clinically relevant option, due to the 311nm peak in the emission spectrum of Hg lamps, which are an inexpensive and widely used light source. Thus, future studies with this system to assess LAGT therapy in vivo are warranted to assess the true potential of this technology.

Conclusions

311nm UV is the optimal wavelength for LAGT based on its remarkably high peak effect (800-fold), its low cytotoxicity, and its inability to induce DNA damage at effective doses. *In vivo*, 311nm UV can significant increase (6.6-fold) rAAV transduction efficiency in articular chondrocytes without evidence of cytotoxicity. These 311nm UV effects correlated with its potent ability to induce intracellular ROS, confirm that this biochemistry is central to the mechanism by which it activates DNA polymerases to facilitate rAAV second-strand synthesis.

Methods

Cell lines and viral stock

Human embryonic kidney HEK 293A (Invitrogen, R705-07) and mouse embryonic C3H10T1/2 (ATCC, CCL-226) adherent cell lines were cultured in standard medium (Dulbecco's modified eagle medium/10% fetal bovine serum/penicillin-streptomycin) and plated in 96-well and 24-well culture plates. The assays were performed at 90% confluence.

The rAAV-Luc vector (rAAV type 2.5 carrying luciferase gene under the cytomegalovirus promoter) was obtained from Gene therapy vector core facility at the University of North Carolina at Chapel Hill.

UV sources

288, 311, 320 and 330nm—A xenon short arc light source (Hamamatsu Photonics, Japan, LC8 150 W) was customized to produce a continuous output of specific wavelength ranges of ultraviolet light for irradiation of cultured cells. A bandpass filter was placed in the beam path after the internal shutter to select the specific wavelengths used in this study. The bandpass filter spectra were measured using a Newport OSM 100 UV/VIS Spectrometer that had a 0.1 nm resolution in the 200–1100 nm spectral region and a wavelength accuracy of +/− 0.08 nm at 349nm. The bandpass filters obtained from Asahi Spectra provided a peak transmission of 65%, with a 10 nm full width at half maximum bandpass centered at the following wavelengths: 288, 311, 320, and 330 nm. These filters were effective in the ultraviolet spectral region, but passed wavelengths longer than 500 nm with little attenuation. A Hoya U340 ultraviolet transmitting filter was added as a shortpass filter to eliminate all output except for the intended bandpass UV emission during the power calibration measurement. Table 1 provides the performance of this illumination source at full output power. The full bandpass power in the UV was then calculated using the known U340 transmission provided in Table 1. All experiments were performed using the Asahi UV bandpass filter only, as the wavelengths > 500 nm were not deemed to produce any adverse effects on the cell cultures. The LC8 provides a power adjustment (1% increments)

and internal shutter (0.1 second resolution) that allowed precisely timed exposures of the cell culture samples. The filtered ultraviolet light output is coupled to a 5 mm diameter multifiber bundle, which had a 1 meter length and an 11 degree half angle beam divergence.

349nm—The 349 nm ultraviolet exposure system used a diode-pumped Nd:YLF laser system, which was frequency shifted to 349 nm (0.1 nm 50% bandwidth) and provided 0–24 × 10-6J pulses at a repetition rate of 5,000 pulses per second. The ultraviolet light was simultaneously coupled through a 200 micron core multimode fiber along with a continuous 532 nm 2 mW alignment laser. A maximum dose of 282 $J/m^2/s$ was obtained for a 19 mm diameter exposure area at full diode pumping current.

365nm—A Hamamatsu LCL1 model L9613-200 UV LED spot curing light source was used to produce a peak centered at 365nm. This source employed a 200 mW, 365 nm (10 nm 50% bandwidth) LED and provided an exposure area of 10 mm diameter at the output of the exposure aperture. The output fluence was adjustable through the control of the percentage of full diode current (1–100%), along with the 0.1 second time duration control (0 to > 1000 seconds) provided by an internal shutter. The maximum fluence produced by this unit was 1 $kJ/m^2/s$.

UV irradiation

The exposure dosage was derived from the values listed in Table 1. The cell culture plate was positioned under the vertically held fiber optic cable. The gap between the fiber and cell plate was adjusted to illuminate either 1 or 4 wells in 96 well plate or 1 well in 24 well plate. The fluence was then calculated from the listed full UV bandpass power, using the specific beam area and the exposure time: $F = P/A \times T \times 10$ (units J/m^2), where P is the UV power from Table 1, A is the area of the UV beam at the cell layer position in cm^2, T is exposure time in seconds and 10 corrects for the unit conversion from mW/cm^2 to J/m^2. The desired doses of specific wavelength ranges were delivered to cells by setting the fiber output at the specified distance and specifying the exposure time that varied from 0.5 seconds to 10 minutes.

Efficacy of light-activated gene transduction (LAGT)

For irradiation, the 90% confluent cultured adherent cells in transparent polystyrene 96 well plates were kept warm on a 37°C heating plate covered with white paper, the medium was replaced with 37°C phosphate buffered saline (PBS). The cells were irradiated with specified wavelength ranges and doses. Each condition was done in 4 replicates. The PBS was replaced with the fresh 37°C warm medium containing the rAAV-Luc virus, to obtain the multiplicity of infection of 1000 virus genomes per cell. Twenty four hour later, the medium was removed, the cells were washed twice with PBS and homogenized in culture plates by intensive orbital shaking (40 rpm at 7 mm diameter) with 25 ul of Cell Lysis Buffer (Promega) and 8 beads in each well (Circonia-Silica, 1 mm, Biospec Products, Bartlesville, OK) for 10 minutes. The lysates were transferred to 96 well black plates, 100 ul of Luciferase Substrate (Promega) was added immediately and quick using Eppendorf repeater, the luminescence was read using Modulus microplate reader (Promega, Sunnyvale CA), 0.5 sec each read, each plate was read 3 times. Statistical analysis of the results shown

in figures 2–6 was performed using one-way analysis of variance with GraphPad InStat (www.graphpad.com).

Cytotoxicity by trypan blue staining

Selective staining of dead cells by trypan blue was used 1 hour after UV irradiation as a measure cytotoxic effects in 90% confluent cells *in situ*29. Staining *in-situ* was used to avoid detachment of cells with trypsin which causes additional damage thus raising the background as observed in “no light” controls. The number of floating cells was controlled with hemocytometer counting and found insignificant even after highly toxic doses of UV. The cells were cultured in 24 well plates, irradiated, incubated for 30 min., covered with a solution of 0.4% trypan blue (Invitrogen) for 30 seconds, the trypan blue solution was aspirated, the cells were immediately photographed with Nikon D40 camera attached to Olympus microscope. Blue and colorless cells were later counted using ImageJ.

Quantification of DNA damage by Comet assay

DNA damage was quantified using single cell gel electrophoresis assay, also known as Comet assay, using the Comet assay kit (Cat. 4250-050-K by Trevigen, Gaithersburg, MD) in accordance with the manufacturer’s protocols. In brief, 293 and C3H cells were irradiated in 96 well culture plates through a layer of PBS, immediately scraped, resuspended, embedded in low-melting agarose on the surface of a microscope slide and lysed by submerging into a lysis buffer. Following 15 min alkaline lysis, the cells were subjected to electrophoresis in alkaline conditions such that the DNA fragmented by UV and alkaline treatments would leave the original location of the cell and migrate in agarose forming a tail. The microscope slides were subjected to electrophoresis under approximately 1–2 mm layer of buffer at 1 V/cm voltage for 25 min. The obtained comets (the remaining DNA in the cells and the tails) were visualized by SYBR green staining and fluorescent microscopy with Olympus microscope. Digital images were obtained with such resolution that an average cell had a diameter of about 150 pixels. The intensities and sizes of the obtained “comet heads” and “tails” were quantified using a free Cometscore program v.1.5 by Tritek, Sumerduck, VA. Fifty or more cell traces per treatment were analyzed. Tail moment calculated by Cometscore program was used for plotting the values as it is a function of both intensity of the tail (amount of migrating DNA) and its relative size (size of DNA fragments). This Tail Moment, commonly named “Olive Tail Moment” 30 is a product of tail length and its relative intensity, where tail relative intensity is calculated relative to total cell intensity and tail length is defined as the distance in pixels between center of the tail and the center of the comet head and represents a measure of DNA damage.

Pyrimidine dimers

The 90% confluent cells in 24 well plates were irradiated with UV light via a layer of PBS. The PBS was replaced with 500ul of lysis buffer containing 100 mM Tris-HCl (pH 8.0), 5 mM EDTA (pH 8.0), 200 mM NaCl, 0.2% SDS and 100ug/ml Proteinase K and incubated at 55°C overnight. DNA was sedimented in rolled tubes with 0.5 ml isopropanol and 200ug of glycogen for 4 hours, centrifuged, dissolved in TE at 55°C for 1 hour, quantified with Nanodrop spectrophotometer (ThermoFisher, Waltham MA) and agarose electrophoresis

and fragmented with EcoRI enzyme for ease of pipetting. Pyrimidine dimers were quantified using Southern-Western dot-blot assay31 with a polyclonal antibody raised against UV-treated DNA (Thymine dimers antibody, Abcam, ab10347). 30ng of DNA from 288nm treatment and 600ng of DNA from 311, 320 and 330nm treatments were denatured by heating 10 min in TE buffer and cooling, loaded on Hybond N+ membrane (GE Healthcare, Piscataway, NJ), baked for 12 min at 80°C, blocked in 5% dry milk, hybridized to the primary antibody, 1:500 dilution, washed, hybridized to the secondary horse-radish peroxidase-conjugated antibody at 1:500 dilution (antimouse HRP, Thermo Scientific, thermoscientific.com), and developed using ECL plus assay (GE Healthcare) and variable time exposures with BioMax film (Kodak, Rochester, NY). Serial dilutions of 254nm UV-treated DNA were used to determine the exposure with linear dynamic range of gray color. The film was scanned and relative spot intensity was measured.

Reactive oxygen species (ROS) assay

Formation of ROS was assayed with a fluorescent probe 2′,7′-dichlorofluorescein-diacetate (DCFH-DA) (Invitrogen, Molecular Probes, Eugene, OR) and flow cytometry as previously described16 with minor modifications. DCFH-DA was prepared in dim light as 5mM stock in methanol of and stored at −20°C. The 90% confluent cells in 24 well plates were irradiated with UV light via a layer of warm (37°C) phosphate buffered saline (PBS). Under dim light, PBS was replaced with a fresh warm (37°C) 200uM DCFH-DA solution in DMEM without serum, the plates were kept in CO2 incubator for 30 min, cells were washed with PBS, covered with 100ul of 0.5% Trypsin (Invitrogen) for 7 min, resuspended in 1.5ml PBS and analyzed with Accuri flow cytometer (Accuri, Ann Arbor, MI) using 450nm excitation and 530nm emission fluorescence measurement.

Effects of UV on light-activated gene transduction in vivo

The effects of 313 nm UV light-activated gene transduction on articular chondrocytes *in vivo* were evaluated in the patellar trochlea defect rabbit model as previously described16,19. Female New Zealand White rabbits (4.5 to 4.7 kg) were studied following protocol approval by the University of Rochester Committee for Animal Resources. Anesthesia was provided by a single intramuscular injection of a mixture of ketamine (35 mg/kg) and xylazine (5 mg/kg). Afterward, a surgical plane of anesthesia was maintained with isoflurane gas (2% to 2.5%). The defect was generated with a 2 millimeter punch after exposing the articular cartilage of the patellar trochlea through an anteromedial parapatellar arthrotomy and lateral luxation of the patella. The defect was exposed to escalating doses of 313 nm UV light delivered to a 6 mm diameter spot centered at the defect via fiberoptic light guide positioned 4 mm above the surface. Previously, we demonstrated that rAAV infection is very efficient, reaching its peak after only ten minutes of direct interaction between the virus and the cells.32 Thus, to deliver the vector to the chondrocytes at the edge of the defect, 10^9 viral genomes of rAAV-eGFP in 80 μL of Hyalgan (sodium hyaluran) gel was gently applied over all open cartilage surface of approximately 1.3 cm^2 with a sterile non-absorbing applicator. The knee capsule and skin were closed in layers. For pain management, the rabbits received 1.1 mg/kg of intravenous Banamine (flunixin meglumine) preoperatively, followed by 1.1 mg/kg of Banamine administered intramuscularly or subcutaneously once a day for two days postoperatively if indicated by clinical signs. The

rabbits were euthanized with pentobarbital 48 hours after LAGT treatment. Both the experimental knee and the uninvolved, contralateral control knee were harvested, decalcified in Formical (Decal Chemical, Tallman, NY), embedded in paraffin, and sectioned into 3-mm sections perpendicular to the articular surface. Immunohistochemical staining was done with goat anti-GFP antibody (Abcam, ab6673) in sections pretreated with Peroxidase I blocking reagent and Background Sniper. Visualization was done with Goat HRP-polymer Detection Kit and Romulin AEC Chromogen (all reagents from Biocare Medical, Concord, CA). The relative content of lacunae and eGFP-positive cells was quantified with use of stereotactic histomorphometry by three reviewers (MMR, FB and EB) who were blinded to the treatment. The reviewers counted the total number of articular chondrocytes, the number of eGFP-positive chondrocytes, and the number of empty lacunae in 40x objective fields in 50 micrometer deep superficial layer of cartilage at 1.5–3mm distance range from the center of the defect. The means of the three scores were used for ANOVA analysis of variance.

Acknowledgments

We thank Vera Gorbunova, Andrei Seluanov and Olga Smirnova for technical advice and Erik R. Sampson, Barbara Stroyer, Echoe Bouta and Calvin Yoon for technical help. This work was funded by LAGeT LLC and a NIH R43 grant (AR57589). The work was conducted at the Center of Institute Ventures at the Institute of Optics at the University of Rochester.

References

1. Evans C, Ghivizzani S, Robbins P. Gene therapy of the rheumatic diseases: 1998 to 2008. Arthritis Research & Therapy. 2009; 11:209. [PubMed: 19232068]
2. Evans C, Ghivizzani S, Robbins P. Orthopedic gene therapy in 2008. Molecular Therapy. 2008; 17:231–244. [PubMed: 19066598]
3. Evans C, Robbins P. Potential treatment of osteoarthritis by gene therapy. Rheumatic Disease Clinics of North America. 1999; 25:333–344. [PubMed: 10356421]
4. Goater J, Muller R, Kollias G, Firestein GS, Sanz I, O'Keefe RJ, et al. Empirical advantages of adeno associated viral vectors in vivo gene therapy for arthritis. J Rheumatol. 2000; 27:983–989. [PubMed: 10782827]
5. Ulrich-Vinther M. Gene therapy methods in bone and joint disorders. Acta Orthopaedica. 2007; 78:2–64. [PubMed: 17453386]
6. Brockes J, Kumar A. Appendage regeneration in adult vertebrates and implications for regenerative medicine. Science. 2005; 310:1919. [PubMed: 16373567]
7. Lee K, Chan C, Patil N, Goodman S. Cell therapy for bone regeneration-Bench to bedside. J Biomed Mater Res B Appl Biomater. 2008; 89:252–263. [PubMed: 18777578]
8. Schwarz EM. The adeno-associated virus vector for orthopaedic gene therapy. Clinical orthopaedics and related research. 2000:S31–S39. [PubMed: 11039749]
9. Ferrari FK, Samulski T, Shenk T, Samulski RJ. Second-strand synthesis is a rate-limiting step for efficient transduction by recombinant adeno-associated virus vectors. Journal of Virology. 1996; 70:3227–3234. [PubMed: 8627803]
10. Fisher KJ, Gao GP, Weitzman MD, DeMatteo R, Burda JF, Wilson JM. Transduction with recombinant adeno-associated virus for gene therapy is limited by leading-strand synthesis. Journal of Virology. 1996; 70:520–532. [PubMed: 8523565]
11. Dai J, Rabie ABM. Gene therapy to enhance condylar growth using rAAV-VEGF. Angle Orthodontist. 2008; 78:89–94. [PubMed: 18193964]
12. Ulrich-Vinther M. Gene therapy methods in bone and joint disorders. Evaluation of the adeno-associated virus vector in experimental models of articular cartilage disorders, periprosthetic osteolysis and bone healing. Acta orthopaedica Supplementum. 2007; 78:1. [PubMed: 17427340]

13. Hauck B, Zhao W, High K, Xiao W. Intracellular viral processing, not single-stranded DNA accumulation, is crucial for recombinant adeno-associated virus transduction. Journal of virology. 2004; 78:13678. [PubMed: 15564477]
14. Alexander I, Russell D, Spence A, Miller A. Effects of gamma irradiation on the transduction of dividing and nondividing cells in brain and muscle of rats by adeno-associated virus vectors. Human gene therapy. 1996; 7:841–850. [PubMed: 8860836]
15. Koeberl DD, Alexander IE, Halbert CL, Russell DW, Miller AD. Persistent expression of human clotting factor IX from mouse liver after intravenous injection of adeno-associated virus vectors. Proceedings of the National Academy of Sciences of the United States of America. 1997; 94:1426–1431. [PubMed: 9037069]
16. Maloney M, Goater J, Parsons R, Ito H, O'Keefe R, Rubery P, et al. Safety and efficacy of ultraviolet-a light-activated gene transduction for gene therapy of articular cartilage defects. The Journal of Bone and Joint Surgery. 2006; 88:753. [PubMed: 16595465]
17. Lemay M, Wood KA. Detection of DNA damage and identification of UV-induced photoproducts using the CometAssay kit. BioTechniques. 1999; 27:846. [PubMed: 10524327]
18. Collins AR. Single cell gel electrophoresis: Detection of DNA damage at different levels of sensitivity. Electrophoresis. 1999; 20:2133–2138. [PubMed: 10451126]
19. Brittberg M, Nilsson A, Lindahl A, Ohlsson C, Peterson L. Rabbit articular cartilage defects treated with autologous cultured chondrocytes. Clinical orthopaedics and related research. 1996; 326:270. [PubMed: 8620653]
20. Bhosale A, Richardson J. Articular cartilage: structure, injuries and review of management. British medical bulletin. 2008; 87:77. [PubMed: 18676397]
21. Hunziker E. Articular cartilage repair: basic science and clinical progress. A review of the current status and prospects. Osteoarthritis and Cartilage. 2002; 10:432–463. [PubMed: 12056848]
22. Bénazet JD, Zeller R. Vertebrate limb development: moving from classical morphogen gradients to an integrated 4-dimensional patterning system. Cold Spring Harbor Perspectives in Biology. 2009:1.
23. Brockes JP. Amphibian limb regeneration: rebuilding a complex structure. Science. 1997; 276:81. [PubMed: 9082990]
24. Kielbassa C, Roza L, Epe B. Wavelength dependence of oxidative DNA damage induced by UV and visible light. Carcinogenesis. 1997; 18:811. [PubMed: 9111219]
25. Demple B, Harrison L. Repair of oxidative damage to DNA: enzymology and biology. Annual Review of Biochemistry. 1994; 63:915–948.
26. Duan D, Sharma P, Dudus L, Zhang Y, Sanlioglu S, Yan Z, et al. Formation of adeno-associated virus circular genomes is differentially regulated by adenovirus E4 ORF6 and E2a gene expression. J Virol. 1999; 73:161–169. [PubMed: 9847318]
27. Zhang Y, Ma WY, Kaji A, Bode AM, Dong Z. Requirement of ATM in UVA-induced signaling and apoptosis. J Biol Chem. 2002; 277:3124–3131. [PubMed: 11723137]
28. Kay ERM, Simmons NS, Dounce AL. An improved preparation of sodium desoxyribonucleate. Journal of the American Chemical Society. 1952; 74:1724–1726.
29. Perry S, Epstein L, Gelbard H. In situ trypan blue staining of monolayer cell cultures for permanent fixation and mounting. BioTechniques. 1997; 22:1020–1024. [PubMed: 9187742]
30. Olive P, Wlodek D, Banath J. DNA double-strand breaks measured in individual cells subjected to gel electrophoresis. Cancer research. 1991; 51:4671. [PubMed: 1873812]
31. Batista L, Roos W, Kaina B, Menck C. p53 Mutant Human Glioma Cells Are Sensitive to UV-C-Induced Apoptosis Due to Impaired Cyclobutane Pyrimidine Dimer Removal. Molecular Cancer Research. 2009; 7:237. [PubMed: 19208740]
32. Ito H, Goater JJ, Tiyapatanaputi P, Rubery PT, O'Keefe RJ, Schwarz EM. Light-activated gene transduction of recombinant adeno-associated virus in human mesenchymal stem cells. Gene therapy. 2004; 11:34–41. [PubMed: 14681695]

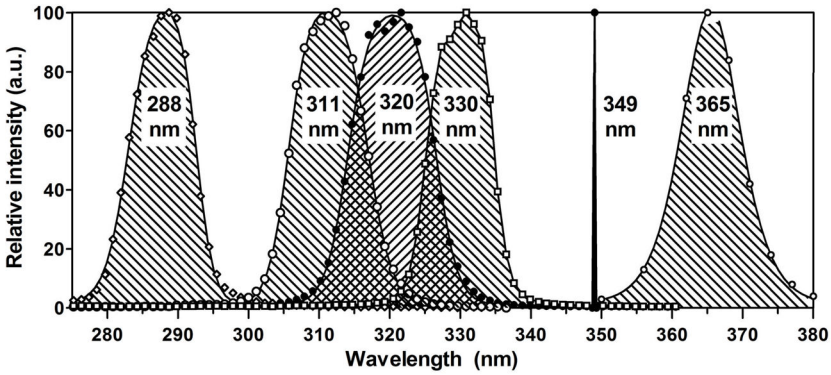

Figure 1. Spectral output of the UV light sources

The relative spectral output from the filtered xenon lamp, Nd:YLF laser, and the UV LED system, are presented at the indicated wavelengths. Note that there is no significant overlap between the UVB system focused at 288nm with the three UVA filtered emissions, while there is significant overlap between the filtered UV focused at 311nm, 320nm, and 330nm. The data are presented as the mean + SE in arbitrary units (a.u.)

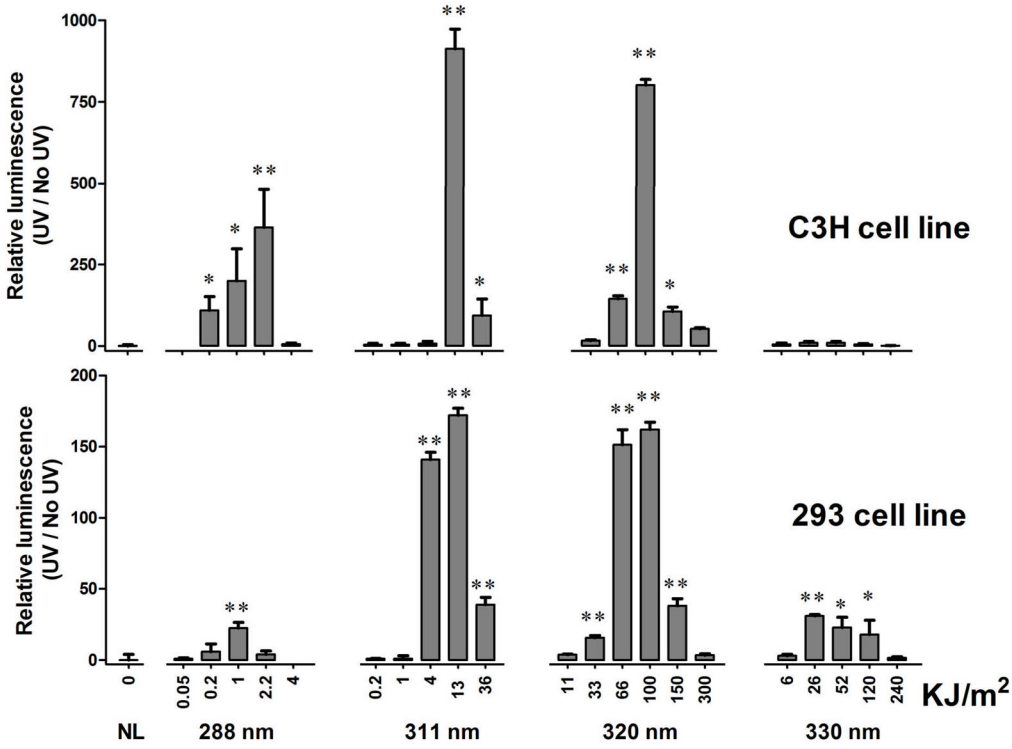

Figure 2. Efficacy of LAGT at the UVB-UVA transition

C3H and 293 cells were cultured in 96-well plates and subjected to LAGT with rAAV-Luc at MOI = 1,000. The wavelength and doses of UV light were varied between treatment groups as indicated. Each treatment was done in quadruplicate. The optimal dose ranges for each wavelength were selected based on preliminary experiments (not shown). Luciferase activity was assayed after culturing the cells for 24 h after the LAGT treatment, and the data from a representative experiment (n=4) are presented as the fold-change (mean + SE) compared to the no light (NL) treatment group (*$p<0.05$ and **$p<0.01$ vs. 0 J/m^2 UV control, NL).

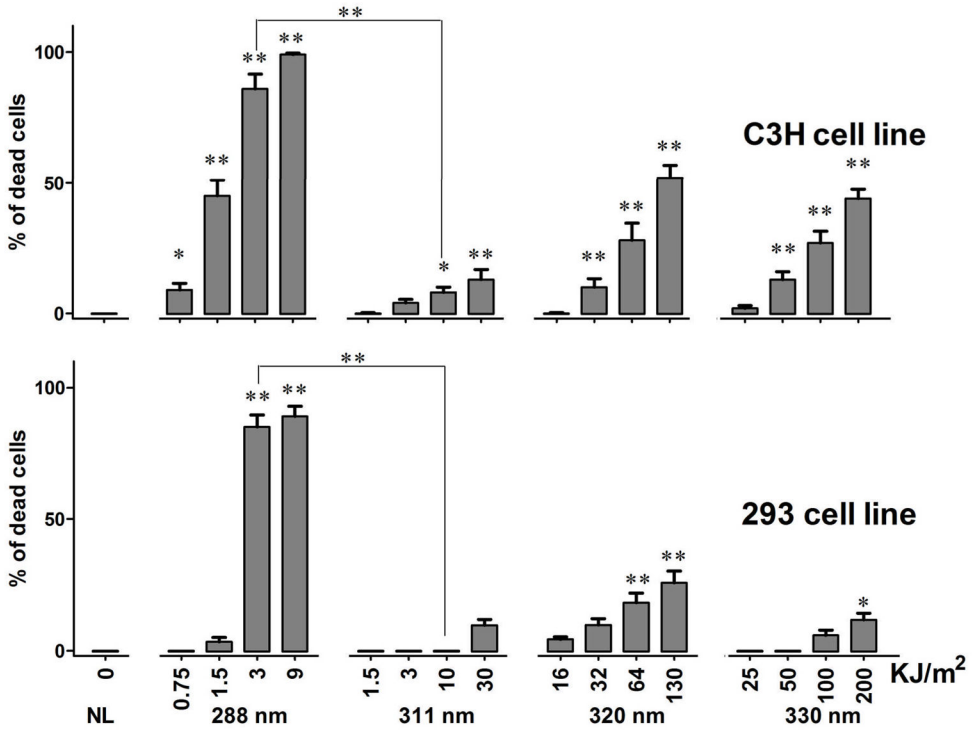

Figure 3. Spectral effects of UV on cell viability

C3H and 293 cells were cultured in 24-well plates and exposed to the indicated fluence of UV in quadruplicate. The cells were then cultured for one hour before Trypan blue staining to assess viability. The percentages (mean + SE) of the stained (dead) cells from a representative experiment (n=4) are presented (*p<0.05 and **p<0.01 vs. no light (NL) control).

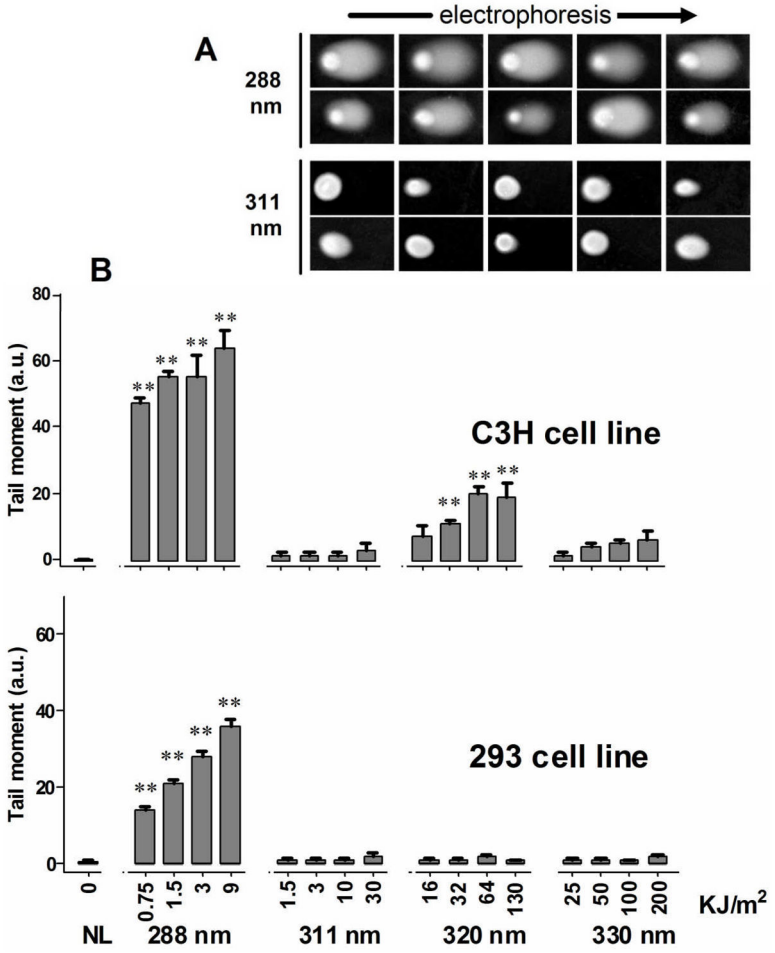

Figure 4. Spectral effects of UV on macroscopic DNA damage (Comet assay)

C3H and 293 cells were cultured in 96-well plates and exposed to the indicated fluence of UV. Single cells were embedded in agarose immediately after UV irradiation, electrophoresed and photographed using a fluorescent microscope to determine the "Olive tail moment" of each cell/comet (representing the extent of DNA damage). (A) Representative photographs of cells from 288 nm (3KJ/m^2) treatment and from 311 nm (10KJ/m^2) treatment. (B) UV action spectrum for "Olive tail moment" in arbitrary units (a.u.). The data are presented as the mean + SE of >50 cells scored for each treatment (**$p<0.01$ vs. no light (NL) control).

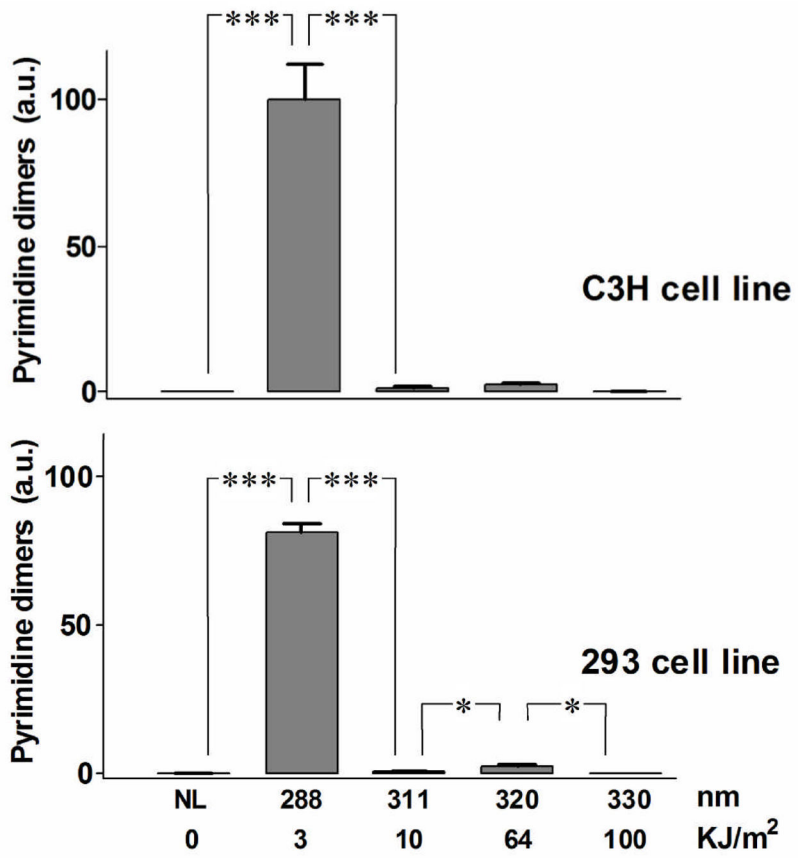

Figure 5. Spectral effects of UV on pyrimidine dimer formation

C3H and 293 cells were cultured in 24-well plates and exposed to the indicated fluence of UV in quadruplicate. Total DNA was isolated from the exposed cells, and pyrimidine dimer levels were determined via dot-blot South-Western assay31. The data from a representative experiment (n=4) are presented in arbitrary units (a.u.) as the mean + SE (*$p<0.05$; ***$p<0.001$ vs. no light (NL) control).

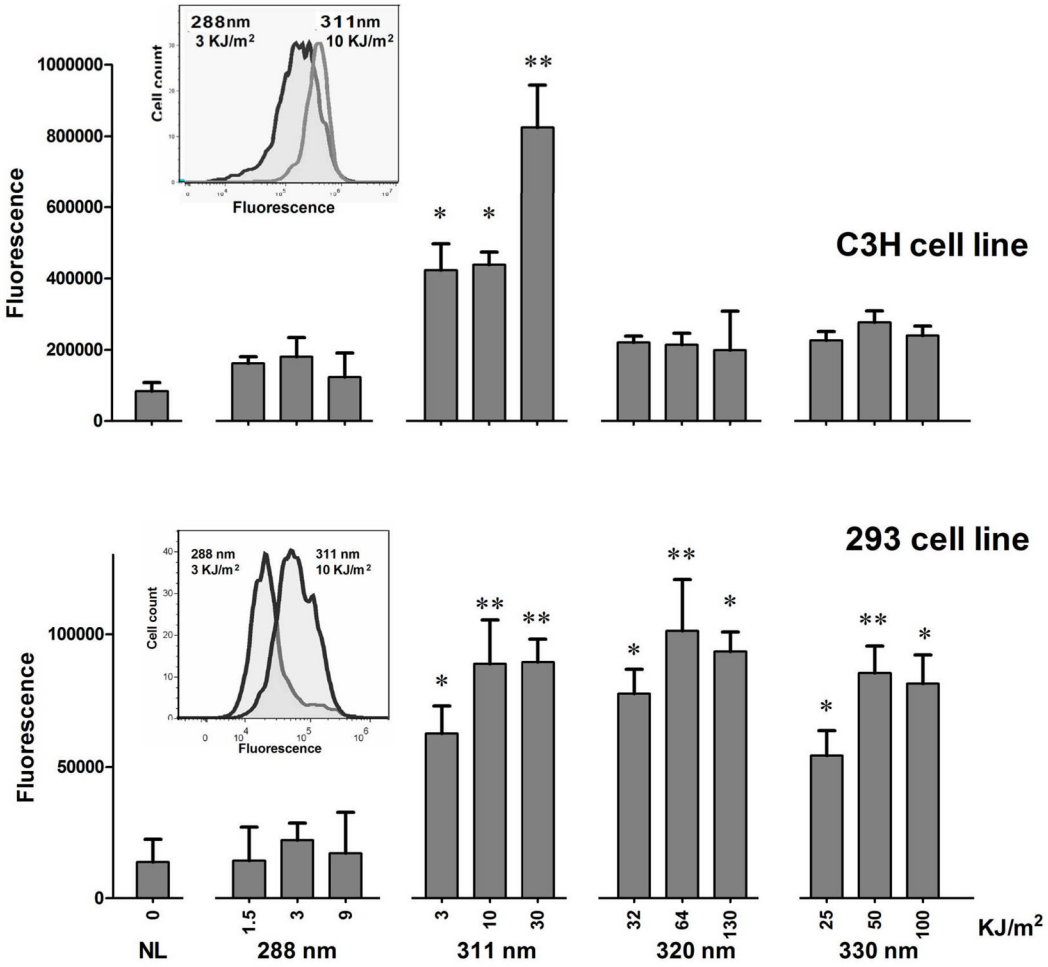

Figure 6. Spectral effects of UV on intracellular ROS generation

C3H and 293 cells were cultured in 24-well plates and exposed to the indicated fluence of UV. Then the cells were incubated with 50uM DCFH-DA in the dark, trypsinized, and the mean fluorescence intensity (MFI) of the culture was determined by flow cytometry. Representative histograms of the 288nm vs. 311nm samples are shown to illustrate the differences observed between these groups. Each bar in the graph represents the mean fluorescence intensity + SE from a representative experiment (n=4; *p<0.05 vs. no light (NL) control).

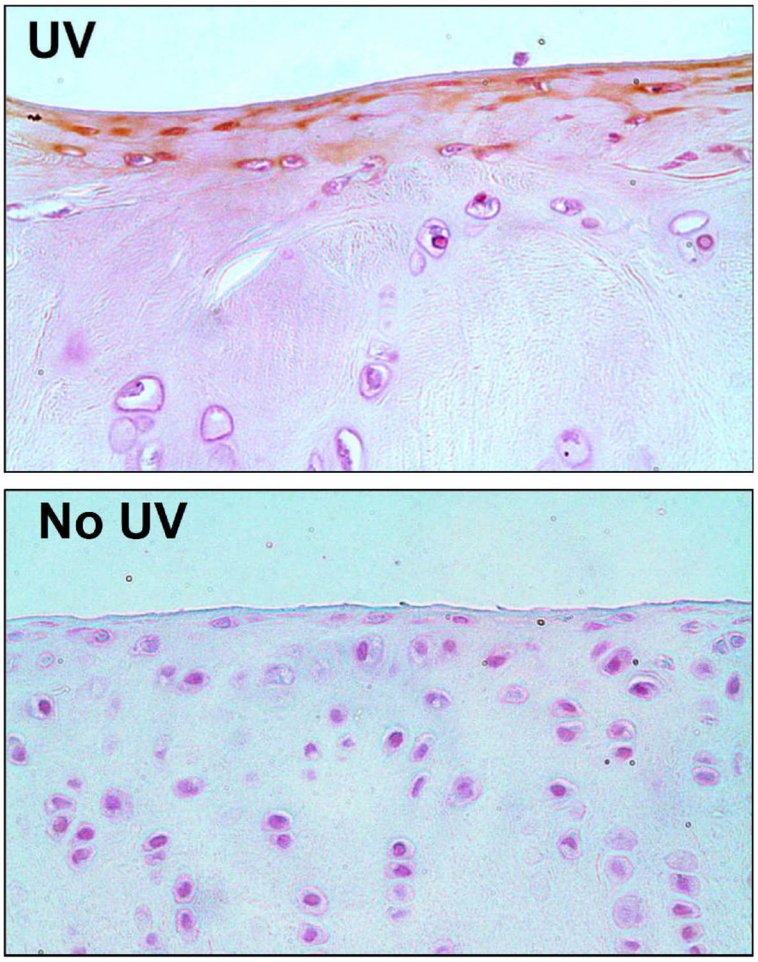

Figure 7. In vivo 311nm UV-induces LAGT in rabbit articular cartilage

Rabbits received defects in their femoral chondyles via open arthrotomy, and the articular surface was irradiated with either 0 (left knee, "No UV") or 6 KJ/m^2 (right knee) of 313 nm UV. Afterwards, the defect was filled with 10^9 viral genomes of rAAV-eGFP in hyalgan gel, and the incision was sutured. The chondyles were harvested 48hrs later, and processed for immunohistochemistry with anti-GFP antibody. A representative section of the LAGT treated (UV) and non-LAGT treated (No UV) area of cartilage outside (0.5 mm away) from the defect are presented at 10x magnification to illustrate the dramatic difference in the number of transduced cells (reddish-brown staining).

Table 1

Bandpass filter center λ (nm)	Power from 5 mm fiber (mW)	Hoya U340 Transmission %	Full UV bandpass output power (mW)	Fluence at 5* mm fiber output (J/m^2/s)
288	5.1	61.3	8.3	424
311	12.9	78	16.5	844
320	16.9	79	21.4	1090
330	13.4	80	16.8	857